Multichannel Double-Row Transmission Line Array for Human MR Imaging at Ultrahigh Fields

Xinqiang Yan, Jan Ole Pedersen, Long Wei, Xiaoliang Zhang*, and Rong Xue*

Abstract*—*Objective: **In microstrip transmission line (MTL) transmit/receive (transceive) arrays used for ultrahigh field MRI, the array length is often constrained by the required resonant frequency, limiting the image coverage. The purpose of this study is to increase the imaging coverage and also improve its parallel imaging capability by utilizing a double-row design.** ***Methods:*** **A 16-channel double-row MTL transceive array was designed, constructed, and tested for human head imaging at 7 T. Array elements between two rows were decoupled by using the induced current elimination or magnetic wall decoupling technique.** ***In vivo*** **human head images were acquired, and g-factor results were calculated to evaluate the performance of this double-row array.** ***Results:*** **Testing results showed that all coil elements were well decoupled with a better than –18 dB transmission coefficient between any two elements. The double-row array improves the imaging quality of the lower portion of the human head, and has low g-factors even at high acceleration rates.** ***Conclusion:*** **Compared with a regular single-row MTL array, the double-row array demonstrated a larger imaging coverage along the z-direction with improved parallel imaging capability.** ***Significance:*** **The proposed technique is particularly suitable for the design of large-sized transceive arrays with large channel counts, which ultimately benefits the imaging performance in human MRI.**

***Index Terms*— Decouple, head, high-field MRI, induced current elimination (ICE), microstrip, multiple row, parallel imaging, parallel transmission (pTx), radio frequency (RF) coil array, RF shimming.**

I. Introduction

ULTRAHIGH field (i.e., 7 T and higher) MRI, could provide a higher signal-to-noise ratio, an improved susceptibility contrast and a greater spectral dispersion [1]–[5]. At the frequency of 300 MHz (Larmor frequency of proton at 7 T) or higher, it is technically challenging to design large-sized head coil [6]–[10] as the wavelength in biological tissue is significant shortened [11]–[13]. Transmit/receive (transceive) arrays have proved to be a popular choice for radio frequency (RF) coil design at ultrahigh fields [14]–[20], providing the capability of RF shimming, parallel transmission (pTx) [21]–[23], and parallel imaging [24]–[27].

Transceive arrays using the microstrip transmission line (MTL) technology have been advocated for ultrahigh field MRI due to the improved resonance stability, reduced radiation losses, and a simple structure [7]–[10], [16], [28]–[37]. However, the image coverage along the coil axis (z-direction) is limited because of the length constrains of regular open-ended MTL resonators at ultrahigh fields, and the reduced B_1 field near the ends of the resonators [8], [38], making usable B_1 along the z-direction often inadequate to cover entire human head. This problem could be addressed by using multiple-row MTL transceive arrays, which are able to provide enough longitudinal coverage by using regular or even shorter MTL elements. With independent transmit elements from different rows, the multiple-row MTL transceive array could offer the possibility of RF shimming and pTx along the z-direction. The multiple-row design could also improve the parallel imaging performance due to the enlarged number of independent receive elements.

The main challenge in designing multiple-row MTL array is to attain sufficient electromagnetic (EM) decoupling among coil elements from adjacent rows. To ensure enough coverage along the z-direction, coil elements from adjacent rows are usually tightly placed, resulting in strongly EM coupling. Although *L/C* decoupling networks [28], [30], [31], [39] have been proposed and shown superior decoupling capability for adjacent elements from the same row, it may not be readily feasible for addressing the strong coupling between elements from adjacent rows.

In this study, we designed and constructed a 16-channel double-row MTL transceive array for human head MR imaging at 7 T. A novel decoupling technique based on the induced current compensation (ICE) or a magnetic wall decoupling method [40]–[45] was employed to reduce the coupling between adjacent rows. To investigate the decoupling performance, transmission coefficient (S_{21}) plots and MR images of two-channel double-row MTL arrays with and without the proposed decoupling method were measured and compared. Bench tests and *in vivo* MR images of the 16-channel dual-row MTL array were obtained to demonstrate its feasibility and performance in

Manuscript received August 8, 2014; revised November 17, 2014 and January 26, 2015; accepted January 30, 2015. Date of publication February 18, 2015; date of current version May 18, 2015. This work was supported in part by the Chinese National Major Scientific Equipment R&D Project under Grant ZDYZ2010-2, in part by the Ministry of Science and Technology of China under Grant 2012CB825500, in part by the National Natural Science Foundation of China under Grant 51228702 and Grant 91132302, in part by the Chinese Academy of Sciences under Grant XDB02010001 and Grant XDB02050001, and in part by the National Institutes of Health, USA, under Grant R01EB008699. *Asterisk indicates corresponding author.*

X. Yan and L. Wei are with the Key Laboratory of Nuclear Radiation and Nuclear Energy Technology, Institute of High Energy Physics, Chinese Academy of Sciences, and also with Beijing Engineering Research Center of Radiographic Techniques and Equipment.

J. Ole Pedersen is with the Sino-Danish Center for Education and Research, University of Chinese Academy of Sciences.

*X. Zhang is with Department of Radiology and Biomedical Imaging, the University of California San Francisco and UCSF/UC Berkeley Joint Graduate Group in Bioengineering, San Francisco, California 94158, USA (e-mail: xiaoliang.zhang@ucsf.edu).

*R. Xue is with the State Key Laboratory of Brain and Cognitive Science, Beijing MRI Center for Brain Research, Institute of Biophysics, Chinese Academy of Sciences, Beijing 100101, China, and also with the , Beijing Institute for Brain Disorders, Beijing 100053, China (e-mail: rxue@bcslab.ibp.ac.cn).

Color versions of one or more of the figures in this paper are available online at http://ieeexplore.ieee.org.

Digital Object Identifier 10.1109/TBME.2015.2401976

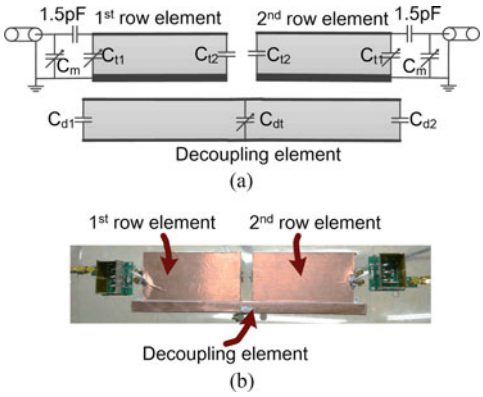

Fig. 1. (a) Equivalent circuit, and (b) photograph of a two-channel double-row MTL array.

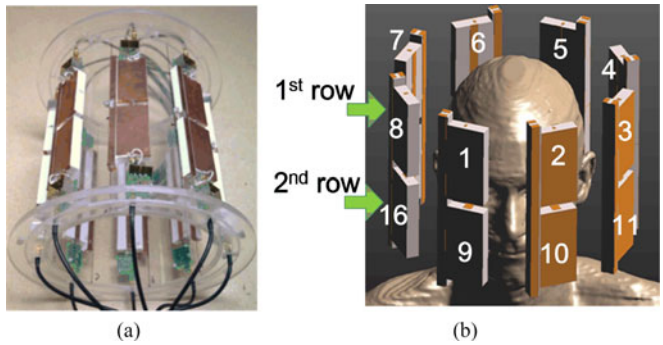

Fig. 2. (a) Photograph of the 16-channel double-row transceive MTL array. (b) Coil elements numbering and layout versus the human head model.

ultrahigh field MRI. Sagittal human head images and g-factors of the double-row array were compared with those of a single-row array to evaluate the benefits offered by the double-row design. The multiple-row design has been applied for traditional *L/C* loop arrays [18], [46]; however, no multiple-row MTL array has been reported to our knowledge.

II. Materials and Methods

A. Two-Channel Double-Row MTL Array

In previous works, ICE decoupling has been successfully applied for MTL resonators [40]–[42], *L/C* loops [43], and monopole antennas [45] to reduce the coupling between adjacent coil elements. In the literature [42], the mutual coupling between the coil element and decoupling element (X^{cd}) has to satisfy a condition to achieve good decoupling performance. The space between two MTL resonators from adjacent rows is very limited and, thus, the decoupling element was placed closely next to the coil elements rather than inserted between them.

Each element in the two-channel double-row MTL array was manufactured from a Teflon bar of 9 cm $\times$ 4 cm $\times$ 1.5 cm, as shown in Fig. 1(a) and (b). The distance between the two elements was 1 cm, and the total length of the double-row MTL array was 19 cm. By using the double row or triple row design with Teflon substrate, the coil length or imaging coverage along the z-direction can reach 60 cm, given a maximum length of $\sim$36 cm for a first harmonic microstrip. The ground was made from adhesive-backed copper foil with a width of 4.5 cm. The strip conductors were made of 10 mm-wide copper tapes. For each MTL element, a trimmer capacitor Ct1 was terminated at the feed end for tuning and a fixed capacitor Ct2 (33pF, ATC Corp, Huntington Station, NY, USA) was terminated at the other end. To avoid the condition that the value of the matching capacitor was too small, a 1.5-pF fixed capacitor and a trimmer capacitor Cm connected in shunt were used for matching [47]. A resonator with two capacitors (Cd1 and Cd2) terminated at both ends and one variable capacitor (Cdt) terminated at the center was applied as the decoupling element.

The reflection coefficient (S_{11}) and transmission coefficient (S_{21}) of the two elements with and without the decoupling element were performed using an Agilent E5071C network analyzer. To assure the performance of the proposed decoupling method, a pattern comparison of MR images on a cylindrical water phantom acquired with: 1) a single-coil element without the other element; 2) one coil element of the coupled two-channel array; and 3) one coil element of the well-decoupled two-channel array; was performed using a gradient recalled echo (GRE) sequence with identical parameters. The parameters of the GRE sequence used were flip angle (FA) = 25°, TR = 100 ms, TE = 10 ms, field of view (FOV) = 210 $\times$ 210 mm^2, matrix = 256 $\times$ 256, slice thickness = 3 mm, bandwidth = 320 Hz/pixel. During the experiments, the cylindrical water phantom (length 37 cm, diameter 16 cm) was placed 3 cm below the coil arrays. The EM parameters of the water phantom were measured by a dielectric probe (DAK-12, SPEAG, Switzerland): conductivity $\sigma = 0.59$ S/m; relative permittivity $\varepsilon_r = 78$.

B. 16-Channel Double-Row Array for Human Head Imaging

The 16-channel double-row human head array consists of eight two-channel blocks as described above. All coil elements were mounted on an acrylic former with an outer diameter of 25 cm. Fig. 2(a) shows the constructed coil array and Fig. 2(b) presents the element numbering.

MTL resonators have demonstrated better decoupling performance over *L/C* loop resonators owing to their confined EM field. Therefore, no extra decoupling method was employed for coil elements from the same row in this study. All coil elements were matched to 50 Ω and tuned to 297.2 MHz, which was the Larmor frequency of the unitized 7-T MRI system. Shielded cable traps were employed to avoid possible "cable resonance."

The scattering (*S*-) parameter matrix of the 16-channel array loaded with a human head was measured with the network analyzer. When any two elements were measured, all other coil elements were terminated with 50-Ω loads. The S_{11} plots were also used to calculate *Q* values. Our RF interface can only operate eight channels, with an eight-way power splitter, eight transmit/receive, switches and eight 50-Ω preamplifiers. To test this 16-channel array, scans were conducted two times. The size of the human head used in this study is about 16 cm in diameter, while the diameter of the coil achieves 25 cm. Phase adjustment is not required when the dimension of the coil array is large compared with the sample size [34]. Therefore, the phase

increment between adjacent channels was set with 45° during each scan. Meanwhile, the unused channels were terminated with 50-Ω loads to eliminate unwanted RF power reflection. During the two scans, the positioning of a subject was carefully kept unchanged via the line markers made on the patient table.

GRE images on a healthy human head were obtained using the 16-channel dual-row array coil. The sequence parameters were set as follows: FA = 25°, TR = 100 ms, TE = 10 ms, FOV = 210 × 210 mm^2, matrix = 256 × 256, slice thickness = 5 mm, number of excitation (NEX) = 1, bandwidth = 320 Hz/pixel. To further evaluate the improved imaging coverage for human head, the obtained sagittal image was also compared with that of a regular single-row eight-channel array coil.

Accelerated GRE images with the reduction factor (*R*) of 2, 3, and 4 were acquired and analyzed to investigate the parallel imaging capability of the 16-channel array structure. The double-row array had a larger number of receive elements, and should have better parallel imaging performance over the regular single-row array. To validate this assumption, g-factor results with accelerations in the anterior–posterior (AP) direction of the 16-channel and eight-channel arrays were measured, calculated, and compared. All MRI experiments were performed on a whole-body MRI scanner (7T MAGNETOM, Siemens Healthcare, Erlangen, Germany). The human MRI experimental protocol was approved by the local Institutional Review Board, and the volunteers signed an informed consent form before MRI experiments. Before human head MR imaging, we performed safety test by measuring the temperature of a piece of 7-kg pork for an hour using the same GRE sequence. The measurement was conducted with an Opsens fiber optic thermometer (Quebec, Canada). We placed four fiber optic sensors separately at shallow and deep regions of the pork meat, and changed the positions for repeated measurements after half hour. The temperature stayed between 21.1° and 21.2° at all selected points, and no "local hot spots" were observed during experiments.

III. Results

A. Bench Test Results and Phantom Images of the Two-channel Double-Row Array

Fig. 3(a) and (b) shows the S_{11} and S_{21} plots of the two MTL elements without decoupling treatments. It is clear that the two elements were strongly coupled ($S_{21} = -7.9$ dB) and the resonant peak was obviously split. By using the ICE decoupling method, the isolation was improved to –25.3 dB and no resonant peak splitting was observed (see Fig. 3(c) and (d), indicating the sufficient decoupling capability of the proposed decoupling method.

Fig. 4 shows the water phantom images acquired from (a) individual elements, (b) elements from the coupled array, and (c) elements from the ICE-decoupled array. Part of the MR signals was obviously transferred to the other coil element when no decoupling treatments were used, as shown in Fig. 4(b), whereas the MR images from the ICE-decoupled array [see Fig. 4(c)] showed great similarity with the images from individual elements [see Fig. 4(a)]. This indicated that the proposed decoupling method could effectively reduce the strong coupling to a sufficient small value, which also validated the *S*-parameter results shown above.

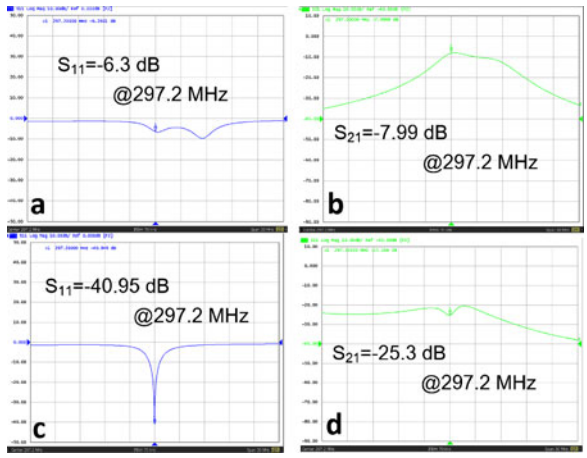

Fig. 3. S_{11} and S_{21} plots versus frequency of the elements from adjacent rows. (a) S_{11} plot without the decoupling element. (b) S_{21} plot without the decoupling element. (c) S_{11} plot with the decoupling element. (d) S_{21} plot with the decoupling element. Better than –25-dB isolation of the two MTL resonators from adjacent rows could be achieved by using the ICE decoupling method.

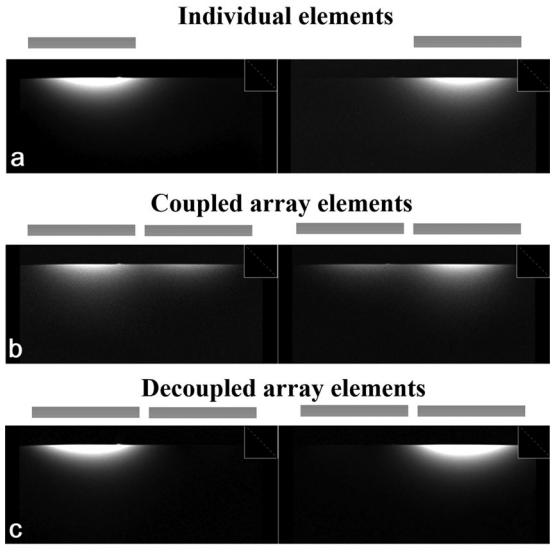

Fig. 4. Water phantom images in the sagittal plane acquired from (a) individual elements, (b) elements from the coupled array (–7.9 dB), and (c) elements from the ICE-decoupled array (–25.3 dB). The parameters of the GRE sequence used were FA = 25°, TR = 100 ms, TE = 10 ms, FOV = 210 × 210 mm^2, matrix = 256 × 256, slice thickness = 3 mm, bandwidth = 320 Hz/pixel. The MR images from the ICE-decoupled array have a similar patterns compared with the images from the individual elements, indicating the excellent decoupling performance.

B. Bench Test Result of the 16-Channel Dual-Row MTL array

Fig. 5 shows the *S*-parameter matrix and noise covariance matrix of the 16-channel double-row MTL transceive array loaded with a healthy human head. The coil numbering in Fig. 5 corresponds to that shown in Fig. 1(b). S_{11} of each coil element was better than –24 dB, indicating all coil elements were well

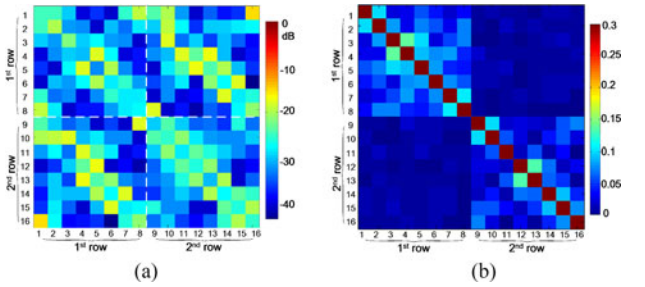

Fig. 5. (a) *S*-parameter matrix and (b) noise covariance matrix of the 16-channel double-row MTL transceive array loaded with a healthy human head. The worst-case isolation among any two elements was –18.1 dB, indicating any two elements of the 16-channel array were well decoupled.

matched to 50 Ω. With the proposed ICE decoupling method, the isolation between two adjacent elements from different rows was better than –20 dB. As expected, the isolation among any two elements of the same row was better than –19 dB even that no extra decoupling treatments were employed. The worst case and average isolation among any two elements of the 16-channel array were –18.1 and –26.7 Db, respectively. The noise covariance results [see Fig. 5(b)] was in agreement with the *S*-parameter results. Given that MR experiments were conducted using the two rows separately (each row one time), the covariance between elements from different rows was almost 0. The unloaded Q of each coil element was approximately 221. The Q value loaded with the human head varied from 92 to 134 due to the different element-sample distance.

C. Transmit Field Profiles, Human Head Images, and Parallel Imaging Performance

Fig. 6(a) shows the transmit field (B_1^+) maps in the transverse (upper panel) and sagittal (lower panel) planes obtained from each row of the double-row array. The B_1^+ maps were calculated by a double-angle method [48] and scaled to angle. Experimental parameters are TR/TE = 1s/10 ms, FA = 10° and 20°, FOV = 210 × 210 mm^2, matrix = 128 × 128 mm^2, slice thickness = 5 mm, bandwidth = 320 Hz. Each row of the double-row array is a standard MTL coil array and demonstrates a typical MTL array property. For the standard single-row MTL arrays, their B_1^+ map of each channel at 7 T has been reported in [16]. The coil sensitivity profiles of individual element of the proposed double-row MTL array were acquired and presented in Fig. 6(b). As expected, the two rows have different B_1^+ and coil sensitivity profiles, which might be advantageous for B_1 shimming and the pTx technology.

Fig. 7(a) and (b) shows the combined sagittal GRE images obtained using the proposed 16-channel double-row array and a regular eight-channel single-row array, respectively. The two arrays have the same length and the sequence parameters for MR imaging are exactly the same. The data of individual elements were combined with the sum of squares (SOS) method and without intensity correction. The double-row array, compared with the regular array, promises a larger imaging coverage, and

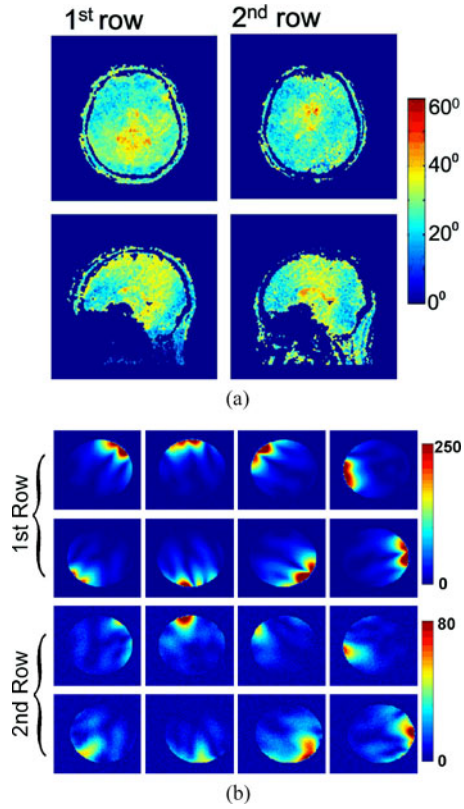

Fig. 6. (a) Transmit field (B_1+) maps of a human brain in the transverse (upper panel) and sagittal (lower panel) planes of each row. (b) Transverse GRE images of individual channels of the double-row MTL array coil for a 7300-ml cylindrical water phantom. The slice was placed in the center of the first row. Imaging parameters are the same as those used in Fig. 6(a). FA = 10°.

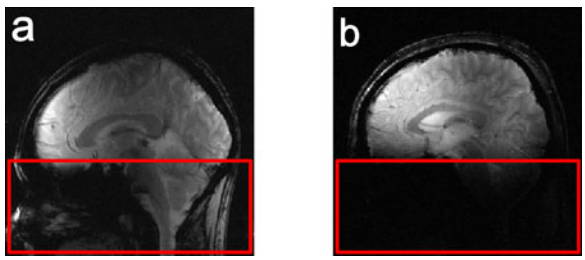

Fig. 7. (a) Sagittal GRE images from the same slice obtained using the 16-channel dual-row array, and (b) the regular eight-channel single-row array. The parameters of the GRE sequence are FA = 25°, TR = 100 ms, TE = 10 ms, FOV = 210 × 210 mm^2, matrix = 256 × 256, slice thickness = 5 mm, NEX = 1, bandwidth = 320 Hz/pixel. The double-row array promises a larger coverage over the regular array, and expands the imaging area to the lower portion of the human head, as shown in the red boxes.

expands the imaging area to the lower portion of the human head, as shown in the red boxes of Fig. 7(a) and (b).

Fig. 8 shows a set of axial GRE images obtained by using each row of the 16-channel array and their combination. It is clear that the signal sensitivity of the first row is high in the upper area of the human head, while very weak at the lower area, e.g., cerebellum, brainstem, and upper spinal cord. With the help of the second row, 16-channel double-row array has the imaging capability of the whole human head. Concluded

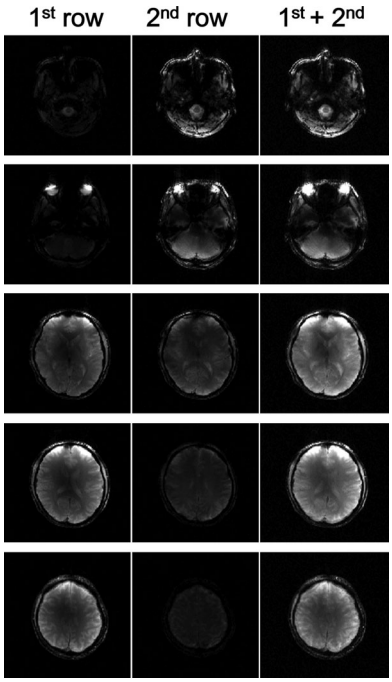

Fig. 8. Set of GRE images of human head in the transverse plane. The imaging parameters are exactly the same as those in Fig. 7.

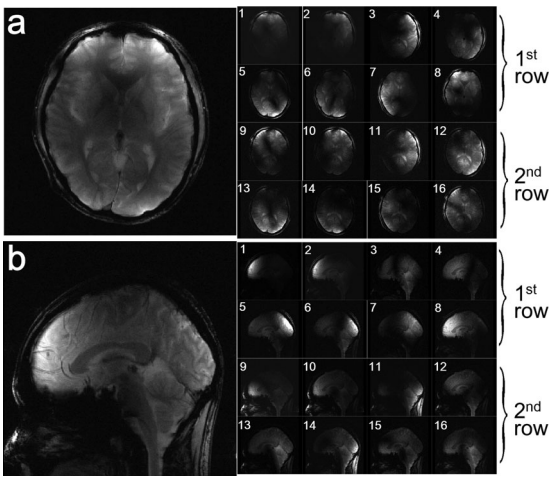

Fig. 9. Individual images from each coil element (right) and their combination with the SOS method (left) in the (a) transverse and (b) sagittal planes.

from the sensitivity profile of each coil element, these axial images have a higher signal sensitivity at peripheral regions and a relatively lower sensitivity in the central area.

Individual images in the transverse and sagittal planes from each coil element and their combination with the SOS method are shown in Fig. 9(a) and (b). These images were reconstructed from raw data and without any postprocessing treatment. Each coil element has a diverse and independent sensitivity map, which is beneficial to enhancing the parallel imaging performance.

To evaluate the parallel imaging performance, sagittal images using the 16-channel array with the reduction rate R of 1 (no acceleration), 2, 3, and 4, respectively are shown in Fig. 10. The accelerated images were reconstructed with generalized autocalibrating partially parallel acquisitions (GRAPPA) using the PULSAR toolbox [49]. In the reconstruction, 18 autocalibration signal (ACS) lines were used for each reduced rate. The image quality is still acceptable when the reduction factor achieves 4.

To further present the improved parallel performance of the double-row design, the average, and maximum g-factors in the sagittal plane using the 16-channel array were measured, calculated, and compared with those from a regular eight-channel array. These average and maximum g-factors with R varying from 2 to 8 are listed in Table I and plotted in Fig. 11(a) and (b). G-factor maps of the two arrays with R of 2, 3, 4, and 5 were also shown in Fig. 11(c). Based on these results, the proposed double-row design, compared with the regular single-row array, improved the g-factors and, thus, parallel imaging performance in the AP direction, even that both arrays have the same number of coil elements in this direction. Considering that there are two elements arranged in the z-direction, the double-row design should also be capable of performing acceleration longitudinally, which is almost impossible for a single-row design. G-factors were calculated using an RF coil array design and analysis software Musaik (Speag, Switzerland).

IV. Discussion

In this study, a MTL transceive array using multiple-row design technique is proposed for ultrahigh field MRI. This technique has been successfully implemented by designing and testing a 16-channel double-row transceive array for human head imaging at 7 T. To reduce the coupling between elements of adjacent rows, a novel decoupling method based on the ICE decoupling method was employed. Given the limited space between elements from adjacent rows, the decoupling element was placed closely next to the coil elements, instead of between them. This decoupling method has shown superior decoupling capability, improving the isolation of the two rows from –7.9 dB (without decoupling treatments) to better than –18 dB.

A main challenge when designing large-sized RF coils at ultrahigh fields is the increased inductance which decreases the resonant frequency. With the proposed multiple-row design, a large imaging coverage was obtained meanwhile the length of each element was significantly shortened. The regular MTL resonator used in RF coil designs is a first harmonic resonator. Its length for resonating at 300 MHz, the proton Larmor frequency at 7 T, is approximately 36 cm when using Teflon as the dielectric substrate. By using the double-row design, the array length could extend to more than 60 cm, which is sufficiently long for most MR applications in humans.

The double-row array has also shown better parallel imaging performance over the regular single-row array because the number of independent receiver elements was doubled. By using the proposed double-row technique, the average g-factor of sagittal human head images was improved from 1.41 to 1.06 at the acceleration rate of 4. The parallel imaging performance could be further improved by increasing the number of rows. In addition, the multichannel multiple-row design provides the capability of

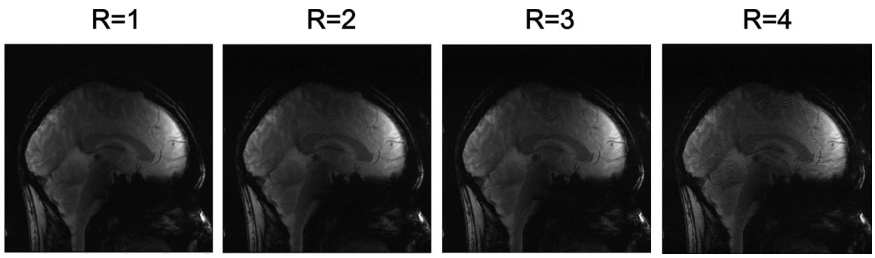

Fig. 10. Reconstructed images of the 16-channel double-row MTL array using GRAPPA with the reduction rate R from 1 (no acceleration) to 4, demonstrating the parallel imaging performance of the proposed double-row MTL array at 7 T. ACS lines = 18.

TABLE I
MAXIMUM AND AVERAGE G-FACTORS AT DIFFERENT REDUCTION FACTORS FOR A REGULAR EIGHT-CHANNEL SINGLE-ROW ARRAY (8CH) AND A 16-CHANNEL DOUBLE-ROW ARRAY (16CH)

Reduction Factor (R)		2	3	4	5	6	7	8
Maximum g-factor	8ch	1.91	2.24	4.37	9.55	38.23	77.61	576.43
	16ch	1.23	1.34	2.02	2.84	3.59	6.30	8.42
Average g-factor	8ch	1.10	1.17	1.41	2.06	4.14	7.46	12.86
	16ch	1.01,	1.02	1.06	1.14	1.29	1.59	1.94

Calculation was based on sagittal human head images. Both the maximum and average g-factors were significantly improved, indicating that the double-row array promises better parallel imaging performance over the single-row array.

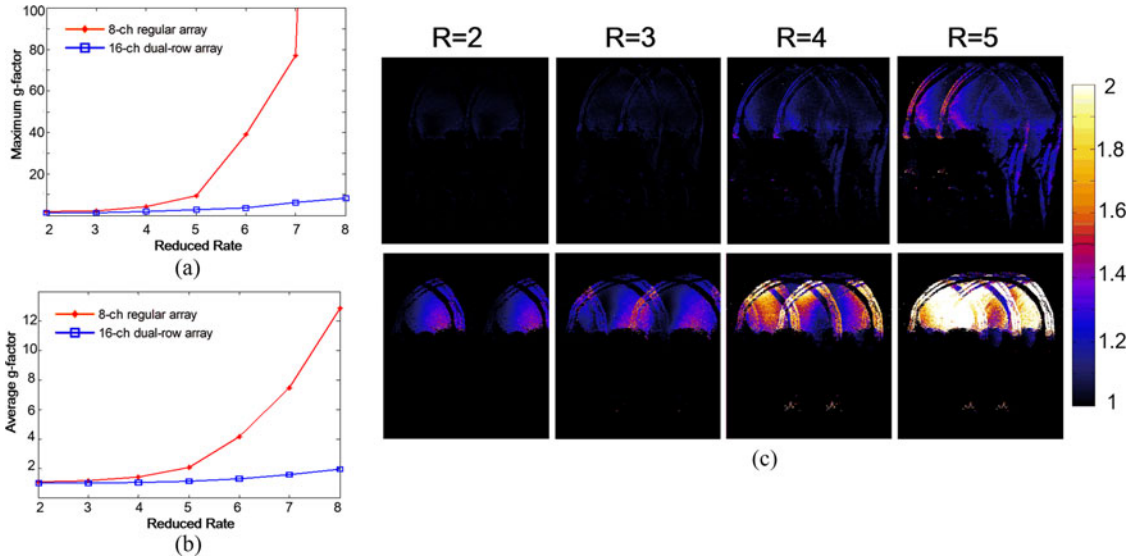

Fig. 11. g-factor results of the 16-channel double-row array and eight-channel single-row array. (a) Maximum and (b) average g-factors with R varying from 2 to 8. (c) g-factor maps of the 16-channel (top row) and eight-channel (bottom row) arrays with R = 2, 3, 4, and 5, respectively. These results indicate that the double-row design could largely decrease the g-factor and, thus, improve the parallel imaging performance.

performing RF shimming and pTx along the z-direction besides the x- and y- directions. Thus it is advantageous in providing more homogeneous transmit field in the human head. By changing the capacitance distribution of coil elements from different rows, different transmit fields and receive sensitivity fields could be obtained [50]. Although in this study, the MTL array with only two rows was tested, the number of rows could extend to three or even more. The double-row MTL array presented here is easy to fabricate in practice, and very suitable for designing large-sized parallel arrays with large channel counts at ultrahigh fields.

V. CONCLUSION

In summary, we proposed a multiple-row transmission line transceive array design for human MR imaging in this study. Its feasibility has been validated through bench tests and *in vivo* MRI experiments at the ultrahigh field of 7 T. The EM

isolation among any two elements achieved –18 dB or better by using the ICE/magnetic wall decoupling method. Compared to the regular single-row MTL array, the double-row array provided larger imaging coverage along the z-direction and better parallel imaging performance, being able to image the whole human brain including the cerebrum, cerebellum, and brainstem.

ACKNOWLEDGEMENT

The authors would like to thank S. Chu and Q. Kong (Institute of Biophysics, Chinese Academy of Sciences), and the RF Department of Siemens, for their assistance and technical support in coil testing.

REFERENCES

[1] E. Yacoub *et al.*, "Imaging brain function in humans at 7 tesla," *Magn. Reson. Med.*, vol. 45, pp. 588–94, 2001.
[2] J. T. Vaughan *et al.*, "7 T versus 4 T: RF power, homogeneity, and signal-to-noise comparison in head images," *Magn. Reson. Med.*, vol. 24, pp. 24–30, 2001.
[3] A. M. Abduljalil *et al.*, "Enhanced gray and white matter contrast of phase susceptibility-weighted images in ultra-high-field magnetic resonance imaging," *J. Magn. Reson. Imag.*, vol. 18, pp. 284–290, Sep. 2003.
[4] H. Lei *et al.*, "*In vivo* 31P magnetic resonance spectroscopy of human brain at 7 T," *Magn. Reson. Med.*, vol. 49, pp. 199–205, 2003.
[5] X. Zhu *et al.*, "Development of (17)O NMR approach for fast imaging of cerebral metabolic rate of oxygen in rat brain at high field," *Proc. Nat. Acad. Sci. USA*, vol. 99, pp. 13194–13199, Oct. 2002.
[6] J. T. Vaughan *et al.*, "High-frequency volume coils for clinical NMR imaging and spectroscopy," *Magn. Reson. Med.*, vol. 32, pp. 206–218, Aug. 1994.
[7] X. Zhang *et al.*, "Microstrip RF surface coil design for extremely high-field MRI and spectroscopy," *Magn. Reson. Med.*, vol. 46, pp. 443–50, Sep. 2001.
[8] X. Zhang *et al.*, "An inverted-microstrip resonator for human head proton MR imaging at 7 tesla," *IEEE Trans. Biomed. Eng.*, vol. 52, no. 3, pp. 495–504, Mar. 2005.
[9] X. Zhang *et al.*, "Higher-order harmonic transmission-line RF coil design for MR applications," *Magn. Reson. Med.*, vol. 53, pp. 1234–1239, May 2005.
[10] X. L. Zhang *et al.*, "A microstrip transmission line volume coil for human head MR imaging at 4 T," *J. Magn. Reson.*, vol. 161, pp. 242–251, Apr. 2003.
[11] Q. X. Yang *et al.*, "Analysis of wave behavior in lossy dielectric samples at high field," *Magn. Reson. Med.*, vol. 47, pp. 982–989, May 2002.
[12] P. F. Van de Moortele *et al.*, "B(1) destructive interferences and spatial phase patterns at 7 T with a head transceiver array coil," *Magn. Reson. Med.*, vol. 54, pp. 1503–1518, Dec. 2005.
[13] T. S. Ibrahim *et al.*, "Design and performance issues of RF coils utilized in ultra high field MRI: Experimental and numerical evaluations," *IEEE Trans. Biomed. Eng.*, vol. 52, no. 7, pp. 1278–1284, Jul. 2005.
[14] R. G. Pinkerton *et al.*, "Transceive surface coil array for magnetic resonance imaging of the human brain at 4 T," *Magn. Reson. Med.*, vol. 54, pp. 499–503, Aug. 2005.
[15] G. C. Wiggins *et al.*, "Eight-channel phased array coil and detunable TEM volume coil for 7 T brain imaging," *Magn. Reson. Med.*, vol. 54, pp. 235–40, Jul. 2005.
[16] G. Adriany *et al.*, "Transmit and receive transmission line arrays for 7 tesla parallel imaging," *Magn. Reson. Med.*, vol. 53, pp. 434–445, Feb. 2005.
[17] K. M. Gilbert *et al.*, "Transmit/receive radiofrequency coil with individually shielded elements," *Magn. Reson. Med.*, vol. 64, pp. 1640–1651, Dec. 2010.
[18] N. I. Avdievich, "Transceiver-phased arrays for human brain studies at 7 T," *Appl. Magn. Reson.*, vol. 41, pp. 483–506, Dec. 2011.
[19] X. Yan *et al.*, "Optimization of an 8-channel loop-array coil for a 7 T MRI system with the guidance of a co-simulation approach," *Appl. Magn. Reson.*, vol. 45, pp. 437–449, 2014.
[20] X. Yan *et al.*, "A monopole/loop dual-tuned RF coil for ultrahigh field MRI," *Quant. Imag. Med. Surg.*, vol. 4, pp. 225–31, Aug. 2014.
[21] Y. D. Zhu, "Parallel excitation with an array of transmit coils," *Magn. Reson. Med.*, vol. 51, pp. 775–784, Apr. 2004.
[22] W. Grissom *et al.*, "Spatial domain method for the design of RF pulses in multicoil parallel excitation," *Magn. Reson. Med.*, vol. 56, pp. 620–629, Sep. 2006.
[23] Z. H. Zhang *et al.*, "Reduction of transmitter B-1 inhomogeneity with transmit SENSE slice-select pulses," *Magn. Reson. Med.*, vol. 57, pp. 842–847, May 2007.
[24] D. K. Sodickson and W. J. Manning, "Simultaneous acquisition of spatial harmonics (SMASH): Fast imaging with radiofrequency coil arrays," *Magn. Reson. Med.*, vol. 38, pp. 591–603, 1997.
[25] K. P. Pruessmann *et al.*, "SENSE: Sensitivity encoding for fast MRI," *Magn. Reson. Med.*, vol. 42, pp. 952–962, 1999.
[26] M. A. Griswold *et al.*, "Generalized autocalibrating partially parallel acquisitions (GRAPPA)," *Magn. Reson. Med.*, vol. 47, pp. 1202–10, Jun. 2002.
[27] D. K. Sodickson *et al.*, "Recent advances in image reconstruction, coil sensitivity calibration, and coil array design for SMASH and generalized parallel MRI," *Magn. Reson. Mater. Phy.*, vol. 13, pp. 158–63, Jan. 2002.
[28] R. F. Lee *et al.*, "Planar strip array (PSA) for MRI," *Magn. Reson. Med.*, vol. 45, pp. 673–683, Apr. 2001.
[29] B. Wu *et al.*, "Design of an inductively decoupled microstrip array at 9.4 T," *J. Magn. Reson.*, vol. 182, pp. 126–32, Sep. 2006.
[30] B. Wu *et al.*, "Capacitively decoupled tunable loop microstrip (TLM) array at 7 T," *Magn. Reson. Imag.*, vol. 25, pp. 418–24, Apr. 2007.
[31] B. Wu *et al.*, "7 T human spine imaging arrays with adjustable inductive decoupling," *IEEE Trans. Biomed. Eng.*, vol. 57, no. 2, pp. 397–403, Feb. 2010.
[32] B. Wu *et al.*, "Multi-channel microstrip transceiver arrays using harmonics for high field MR imaging in humans," *IEEE Trans. Med. Imag.*, vol. 31, no. 2, pp. 183–91, Feb. 2012.
[33] B. Wu *et al.*, "Flexible transceiver array for ultrahigh field human MR imaging," *Magn. Reson. Med.*, vol. 68, pp. 1332–8, Oct. 2012.
[34] G. Adriany *et al.*, "A 32-channel lattice transmission line array for parallel transmit and receive MRI at 7 tesla," *Magn. Reson. Med.*, vol. 63, pp. 1478–1485, Jun. 2010.
[35] G. Adriany *et al.*, "A geometrically adjustable 16-channel transmit/receive transmission line array for improved RF efficiency and parallel imaging performance at 7 tesla," *Magn. Reson. Med.*, vol. 59, pp. 590–597, Mar. 2008.
[36] X. T. Zhang *et al.*, "From complex B-1 mapping to local SAR estimation for human brain MR imaging using multi-channel transceiver coil at 7 T," *IEEE Trans Med. Imag.*, vol. 32, no. 6, pp. 1058–1067, Jun. 2013.
[37] X. T. Zhang *et al.*, "Complex B1 mapping and electrical properties imaging of the human brain using a 16-channel transceiver coil at 7 T," *Magn. Reson. Med.*, vol. 69, pp. 1285–1296, May 2013.
[38] D. O. Brunner *et al.*, "A symmetrically fed microstrip coil array for 7 T," in *Proc. 15th Sci. Meet., Int. Soc. Magn. Reson. Med.*, 2007, p. 448.
[39] B. Wu *et al.*, "Design of an inductively decoupled microstrip array at 9.4 T," *J. Magn. Reson.*, vol. 182, pp. 126–132, Sep. 2006.
[40] Z. Xie and X. Zhang, "A novel decoupling technique for non-overlapped microstrip array coil at 7 T MR imaging," in *Proc. 16th Sci. Meet., Int. Soc. Magn. Reson. Med.*, Apr. 2008, p. 1068.
[41] Z. Xie and X. Zhang, "An eigenvalue/eigenvector analysis of decoupling methods and its application at 7 T MR imaging," in *Proc. 16th Sci. Meet., Int. Soc. Magn. Reson. Med.*, Apr. 2008, p. 2972.
[42] Y. Li *et al.*, "ICE decoupling technique for RF coil array designs," *Med. Phys.*, vol. 38, pp. 4086–4073, 2011.
[43] X. Yan *et al.*, "7 T transmit/receive arrays using ICE decoupling for human head MR imaging," *IEEE Trans. Med. Imag.*, vol. 33, no. 9, pp. 1781–1787, Sep. 2014.
[44] X. Yan *et al.*, "Design and test of magnetic wall decoupling for dipole transmit/receive array for MR imaging at the ultrahigh field of 7 T," *Appl. Magn. Reson.*, vol. 46, pp. 59–66, 2015.
[45] X. Yan *et al.*, "Magnetic wall decoupling method for monopole coil array in ultrahigh field MRI: A feasibility test," *Quant. Imag. Med. Surg.*, vol. 4, no. 2, pp. 79–86, 2014.
[46] G. Shajan *et al.*, "A 16-channel dual-row transmit array in combination with a 31-element receive array for human brain imaging at 9.4 T," *Magn. Reson. Med.*, vol. 71, pp. 870–879, Feb. 2014.

[47] T. Vaughan *et al.*, "9.4 T human MRI: Preliminary results," *Magn. Reson. Med.*, vol. 56, pp. 1274–1282, Dec. 2006.
[48] E. K. Insko and L. Bolinger, "Mapping of the radiofrequency field," *J. Magn. Reson. Ser. A*, vol. 103, pp. 82–85, Jun. 1, 1993.
[49] J. X. Ji *et al.*, "PULSAR: A MATLAB toolbox for parallel magnetic resonance imaging using array coils and multiple channel receivers," *Concept Magn. Reson. B*, vol. 31B, pp. 24–36, Feb. 2007.
[50] X. Yan *et al.*, "Optimization of B1 field homogeneity along the longitudinal direction for 7 T MTL resonators by using a multi-row design," in *Proc. 22th Sci. Meet., Int. Soc. Magn. Reson. Med.*, 2014, p. 1309.

Xinqiang Yan received the B.S. degree from Lanzhou University, Lanzhou, Gansu, China, in 2009, and the Ph.D. degree in particle physics and nuclear physics from the Institute of High Energy Physics, Chinese Academy of Sciences, Beijing, China, in July 2014.

In 2011, he joined the Radiofrequency (RF) Group of the Institute of Biophysics, Chinese Academy of Sciences, Beijing, where he developed RF coils and RF/analog circuits for the commercial Siemens 7-T MR scanner and the ongoing project to construct the first 9.4-T human MRI system of China. At the end of 2014, he moved to Vanderbilt University, Nashville, TN, USA, where he is currently a Postdoctoral Research Fellow at the Institute of Imaging Science and Department of Radiology. His research interests include novel RF coil design, electromagnetic field calculation, and parallel transmit array.

Rong Xue received the B.E. degree in electrical engineering from Tsinghua University, Beijing, China, the M.S. degree in biomedical engineering from Ohio State University, Columbus, OH, USA, and the Ph.D. degree in biomedical engineering from Johns Hopkins University, Baltimore, MD, USA.

She was a Pre- and Post-doctoral Fellow and a Research Associate with the Department of Radiology, Johns Hopkins, developing novel MRI technologies including DTI and 3-D fiber tractograph in high-field MRI systems. She joined the Center for Biomedical Imaging, New York University, as a Research Engineer in 2005, and worked on high-field RF technology in the 3- and 7-T whole-body MRI systems. She has been a Professor with the State Key Laboratory of Brain and Cognitive Science at the Institute of Biophysics, Chinese Academy of Sciences, Beijing, China, since 2007. Her research interests include high-field MR technology, parallel transmission and reception, functional MRI in cognitive and neuroscience studies, application of MR technologies to various human and animal models with different diseases. She has authored and coauthored more than 25 peer-reviewed journal papers and more than 50 conference proceedings in the field of high-field magnetic resonance imaging. She has been a Member of ISMRM since 1997.

Jan Ole Pedersen received the B.S. degree in nanotechnology from Aalborg University, Aalborg, Denmark, in 2012, and the double M.S. degree in neuroscience and neuroimaging from Aarhus University, Aarhus, Denmark, and the University of Chinese Academy of Sciences, Beijing, China, in 2014. He is currently working toward the Ph.D. degree in collaboration with the Technical University of Denmark, Kgs. Lyngby, Denmark, the Sino-Danish Center for Education and Research, Aarhus, and the Danish Research Center for Magnetic Resonance, Aarhus.

The goal of the Ph.D. is to encode non-MRI data into MR images for various applications, such as motion correction and simultaneous EEG and MRI measurements. His research interests include ultra-high field MRI, motion correction, and integration of MRI with other modalities.

Xiaoliang Zhang received the B.E. degree in electrical engineering from the South China University of Technology, Guangzhou, China, and the Ph.D. degree in biomedical engineering from the University of Minnesota, Minneapolis, MN, USA.

He was with the Ohio State University, Columbus, developing the world's first ultrahigh field 8-T whole-body MRI system. Prior to joining the Center for MR Research at the University of Minnesota in 1999, he was employed by Picker International (currently Philips Medical Systems) working on the initial clinical 3-T MR project. He was an Assistant Professor with the Department of Radiology, University of Minnesota. In 2006, he moved to the University of California San Francisco (UCSF), San Francisco, CA, USA, where he is currently an Associate Professor, a core Faculty Member of UC Berkeley and UCSF Joint Graduate Group in Bioengineering, and a Faculty Member of the California Institute for Quantitative Biosciences. His research interests include new methods for magnetic resonance imaging, high-field MR technology, heteronuclear MR, interventional MRI, and their *in vivo* applications. He has authored and coauthored more than 200 peer-reviewed journal papers, conference papers, and book chapters in the field of magnetic resonance imaging.